Thermolysis of Polyphosphazenes. 2. NMR Study of the Kinetics and the Mechanism of the Rearrangement of Poly(dimethoxyphosphazene)

Tai C. Cheng,* Virgil D. Mochel,* Harold E. Adams, and Trent F. Longo

The Firestone Tire & Rubber Company, Central Research Laboratories, Akron, Ohio 44317.
Received April 20, 1979

ABSTRACT: The kinetics of the thermolysis of poly(dimethoxyphosphazene) has been studied by ^{13}C and ^{31}P NMR. The migration of the methyl group from the phosphorus to the nitrogen is conveniently followed by ^{13}C NMR in bulk samples of the cyclic trimer, the cyclic tetramer, and the polymer. All of the intermediate stages of rearrangement are readily observed in the trimer. Upon complete rearrangement, a random distribution of the two possible configurations is observed. The tetramer and the polymer both appear to have but one configuration. ^{31}P NMR is used to confirm the conformations and the configurations of the rearranged products. The kinetic data show there is an induction period the length of which appears to be related to incompletely derivatized phosphorus sites, and the rearrangement is autocatalytic. Activation energies are the same within experimental error for the three materials, indicating that the methyl migration proceeds by the same reaction coordinate. A general mechanism is suggested to explain the induction period and the autocatalytic behavior observed for the migration of the methyl group. An additional mechanism is proposed to account for the scissions and cross-linking observed in the polymer. There is roughly a one-to-one correspondence of the methyl migration and the number of scissions.

Fluorinated alkoxyphosphazene elastomers have generated considerable interest because of their solvent resistance and a temperature service range of -80–400 °F. Aryloxyphosphazenes have also found use in the areas of coatings and insulations because of their low flammability and flame retardance. However, nonfluorinated alkoxyphosphazene polymers have not been commercially developed because of their relatively low thermal stability.

Previous investigators[1] have suggested that this low thermal stability of the poly(alkoxyphosphazenes) is due to the rearrangement as shown:

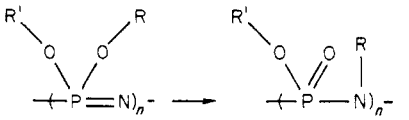

I II

However, conclusive evidence to support this hypothesis has been lacking. In a previous paper[2] we showed by ^{13}C NMR that this rearrangement does take place in the case of poly(dimethoxyphosphazene), as well as in the cyclic tetramer. Results of kinetic studies of the thermolysis of the dimethoxy trimer, tetramer, and polymer will be presented in this paper. Viscosity measurements which suggest a direct correspondence between the observed molecular weight degradation and the rearrangement will be presented and discussed. A mechanism consistent with the rearrangement in all three materials and also the scission and the cross-linking observed in the polymer is proposed.

Experimental Section

General. The preparations of the phosphazene derivatives were carried out under a nitrogen atmosphere. The solvents used for this study were redistilled from either sodium dispersion or calcium hydride. $(NPCl_2)_3$ and $(NPCl_2)_4$ were purchased from the Inabata Co. of Japan and were purified by sublimation. Sodium methoxide was prepared by the reaction of sodium metal and methanol in THF–methanol. The sodium methoxide solution was then dried by letting it stand over 3A molecular sieves at least overnight. The final solutions contained less than 100 ppm of water by Karl Fischer titration.

Synthesis of Methoxy Substituted Cyclophosphazene Compounds. The following procedure for the synthesis of hexamethoxycyclotriphosphazene will serve to illustrate the general method for cyclic phosphazene compounds.

A solution of hexachlorocyclotriphosphazene (50 g, 0.144 mol) in 300 mL of dry hexane was added slowly to a stirred solution of sodium methoxide prepared from 23 g (1 g/atom) of sodium and 200 g (6.25 mol) of methanol in THF. An exotherm raised the reaction temperature to about 60 °C. Refluxing was continued for an additional 9 h. Upon cooling, the reaction mixture was quenched with 300 mL of distilled water. The organic layer was then isolated by the extraction of the reaction mixture with ether three times (500 mL of ether each time). The combined ether layer after being washed with water twice was dried over $MgSO_4$ overnight. After filtration, a white solid material was isolated by evaporation of organic solvents. The yield of this product is 25 g (54%). The trimer had a chlorine content of 0.03 wt %. The chlorine content of the tetramer was 0.11 wt % for preparation 1 and 0.02 for preparation 2.

Synthesis of Poly(dimethoxyphosphazene). The poly(dimethoxyphosphazene) prepared as described in ref 2 has a molecular weight of 220 000 as estimated by DSV measurements. It has a glass transition temperature of -78 °C. The total chlorine content was found to be less than 0.1 wt %.

NMR. ^{13}C NMR measurements were carried out with a JEOL PFT 100 Fourier transform NMR spectrometer operating at 25.15 MHz for ^{13}C nuclei. Spectra were proton decoupled with a heteronuclear white-noise decoupler. Spectra were run at elevated temperatures on the bulk samples in 10 mm o.d. NMR tubes sealed under a vacuum of about 10^{-5} mm. The deuterium external locking system was used for field stabilization.

Spin–lattice relaxation times, T_1, were measured at the temperatures of the kinetic measurements, using the partially relaxed Fourier transform technique. The longest T_1 (listed in the figure captions) in each spectrum was used to choose appropriate ^{13}C frequency pulse widths and repetition times such that all nuclei would be fully relaxed before the ensuing pulse to ensure quantitative results. Nuclear Overhauser Enhancement (NOE) measurements were also made at the temperatures of the kinetic measurements. ^{31}P NMR measurements were carried out with a JEOL FX60Q spectrometer operating at a frequency of 24.15 MHz for ^{31}P nuclei. All ^{31}P spectra were obtained with the protons decoupled to eliminate long-distance coupling effects.

NMR Results

In ref 2 we showed that ^{13}C NMR is a convenient tool to follow the thermally-induced methyl migration, i.e., I → II, in the dimethoxyphosphazene (R′ = R = CH_3) cyclic tetramer and polymer. One of the advantages of the ^{13}C NMR method is that the thermolysis kinetics can be studied directly in the bulk material. We have found that ^{31}P NMR can provide valuable confirming evidence and additional information not available from ^{13}C NMR.

0024-9297/80/2213-0158$01.00/0

Table I
Chemical Shift Positions of ^{13}C NMR Peaks for $[NP(OCH_3)_2]_n$

	peak positions, ppm, for peak no.						
	7	6	5	4	3	2	1
trimer ($n = 3$)	54.09	52.50	33.08	31.3	30.95	29.74	28.35
tetramer ($n = 4$)	53.43	52.46				33.66	33.04
polymer	53.82	52.50				33.86	?

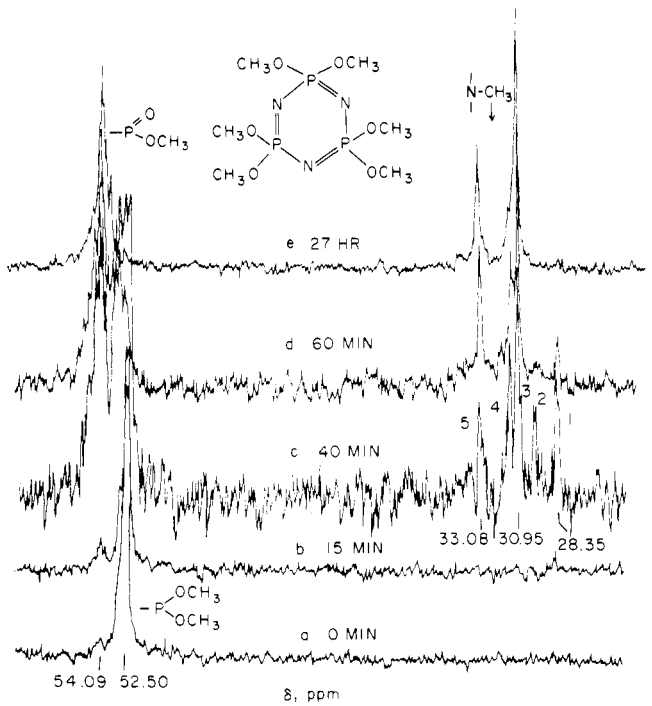

Figure 1. ^{13}C {^1H} NMR spectra at 25.14 MHz following the progress of the thermolysis of $[NP(OCH_3)_2]_3$ at 140 °C. Spectra were run on a neat sample in a sealed, evacuated tube with a repetition time of 2 s and a 45° pulse. (Longest T_1 = 4.9 s at 140 °C.) Peak positions are referenced to external Me_4Si: (a) before heating; (b) after 15 min; (c) after 40 min; (d) after 60 min; (e) after 27 h.

Cyclic Trimer. ^{13}C NMR. The thermolysis of the cyclic trimer, III, was studied over the temperature range

III

120–150 °C. The ^{13}C NMR spectra in Figure 1 show the course of the rearrangement of the cyclic trimer at 140 °C.

Peak positions in ppm referenced to Me_4Si are given in Table I for the cyclic trimer, the cyclic tetramer, and the polymer. The numbering of the peaks for the trimer corresponds to those in Figure 1. It is seen that the original peak (peak 6) in each of the samples has the same shift position. Gated decoupling experiments show that all peaks, before and after rearrangement, are due to methyl carbons, i.e., all show quartet structure when coupled. The assignment of the peaks at about 28–33 ppm to the nitrogen methyl is supported by somewhat related model compounds all of which have NCH_3 resonance peaks in that range[2] and hexamethylphosphoramide which has a chemical shift of 36.8 ppm.[3] In this example, the coupling between the phosphorus and the carbon nucleus is 3.5 Hz. This gives an indication of the magnitude of the coupling constants expected in the phosphazene samples.

In the phosphazene trimer, when the methyl carbon has migrated to the adjacent nitrogen, it becomes very sensitive

Chart I

Monorearranged Structures (2 peaks)

IV (anti to P=O)

V (syn to P=O)

Di- and Trirearranged Structures (3 peaks)

VI

VII (anti to P=O)

VIII (syn to P=O)

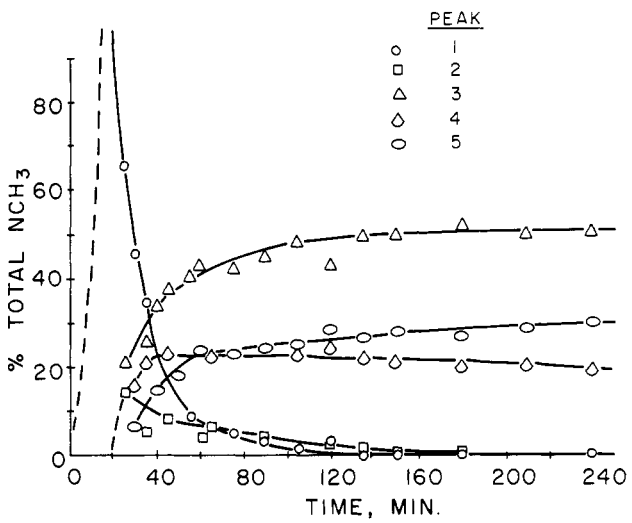

Figure 2. Percent of total NCH_3 resonance vs. time for $[NP(OCH_3)_2]_3$ at 140 °C using peak heights.

to its through-space electronic environment, showing all five of the possible stereo and rotational placements as shown in Chart I. The methoxy carbon remaining on the phosphorus also reflects the change in its environment, but it is far less informative.

Figure 1a displays a single methoxy carbon peak at 52.50 ppm at the start of the heating. After being heated for about 15 min, a peak appears at 28.35 ppm which is due to rearrangement of the first methyl group on a trimer molecule to form either structure IV or V. The numbering of the peaks in the figures corresponds to that shown in structures IV–VIII. A new resonance also appears slightly downfield (54.09 ppm) of the main methoxy peak due to the methoxy which is geminal to the double-bonded oxygen.

With continued heating, four more peaks develop in the NCH_3 region as shown in Figure 1c. The relative intensities of these five peaks vary with further heating until

only three remain, as shown in Figure 1d,e. This is also shown in Figure 2, in which the relative peak heights expressed as percent of the total NCH_3 resonance are plotted vs. time. Peak heights were chosen rather than integrated intensities because of the difficulty of resolving peaks 3 and 4.

The method of presenting the data in Figure 2 might be somewhat misleading. For example, at first glance it appears that peak 1 is the most intense peak. Actually it is the first peak to appear and so represents 100% of the total NCH_3 resonance. Dotted lines have been added to the curves of peaks 1 and 2 to show that in reality they go through a maximum after which they drop off to zero intensity. Peak 4 builds to a nearly constant value but drops off slightly (from 22.5 to 19%) as peaks 3 and 5 increase to constant values.

An interesting conclusion which can be drawn from Figures 1 and 2 is that the relative rates of migration for the mono-, di- and trirearranged species must all be of the same order of magnitude. If the trirearranged rate were very fast compared with those of the intermediate steps, for example, peaks 1 and 2 would not be observed. This latter situation apparently prevails in the case of the tetramer, as will be seen later.

Peaks 1 and 2 are assigned to the NCH_3 carbons of structures IV and V since they appear first and then die out. These structures are present first in the monorearranged product but also are present in the direarranged product. Intuitively, peak 1 would probably be assigned to structure V because it seems energetically more likely than the migration followed by rotation necessary for structure IV. However, it is assigned to structure IV as shown for chemical shift reasons explained below.

When the second methyl group in the same trimer molecule migrates to the nitrogen, three new peaks are introduced as shown in structures VI, VII, and VIII. No new structures are possible when the third methyl is rearranged. Therefore, as the rearrangement proceeds to completion (50% of the methyl rearranged), only three peaks should remain as is observed.

The tallest peak in the spectrum, peak 3, is assigned to the NCH_3 carbon in structure VI because the chemical shift of the NCH_3 carbon in this structure is the same whether the methyl group is "up" or "down". Therefore, it would be expected to have the greatest intensity. The reason for assigning peaks 1 and 2 as described above is that the methyl group 2 in structure V should have an environment more similar to that in structure VI than that of the methyl group 1. Peak 2 is upfield from peak 3 by just 1.2 ppm.

In both di- and trirearranged products, structures VII and VIII are possible. Peaks 4 and 5 are assigned to structures VII and VIII, respectively, by virtue of the fact that by analogy with peaks 1 and 2, in going from anti to syn, a downfield shift of 1.4 ppm is observed. Peak 5 is about 1.8 ppm downfield from peak 4, which is fair agreement.

In the trirearranged trimer, two possible configurations exist: one in which the OCH_3 groups are all on the same side of the ring as shown in configuration IX, and the other in which two OCH_3 groups are on one side and one on the other side as shown in configuration X. For the sake of clarity the ring is shown as a planar triangle in these structures. In reality, of course, the bond angles are considerably different from those depicted. An X-ray diffraction study by Ansell and Bullen[4] has shown that the P–N(CH_3)–P array in the completely rearranged species, i.e., the phosphazane structure, is nearly planar in the solid

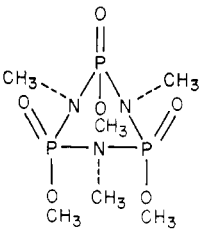

IX

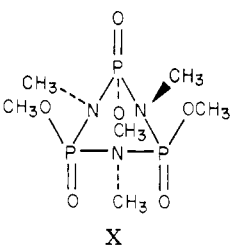

X

state. It has a trans arrangement of the phosphoryl groups as depicted in configuration X. Furthermore, it was found to have a twisted boat conformation with one phosphoryl group occupying the flagpole position and the other two occupying axial positions. The ^{13}C resonances of the methyl carbons on the nitrogens would be expected to be sensitive to these differences in environments presented by the neighboring groups.

In configuration IX a combination of structures VII and VIII is possible, including having all NCH_3's on one side of the ring or the other. For a random placement one would expect equal intensities of the NCH_3 peaks in structures VII and VIII. In the case of configuration X, however, one would expect to observe a constant ratio of 2 to 1 of NCH_3 in structure VI compared with NCH_3 in structures VII and/or VIII. In comparing the curves in Figure 2, we see that the heights of peaks 3 and 5 maintain approximately that 2 to 1 ratio throughout the course of the rearrangement. The two curves run more or less parallel. Peak 4 rises more quickly to about 22%, maintains this level, and slowly drops off. Therefore, it is not likely that this peak is related to peak 3. These considerations strongly suggest that peak 4 is due to configuration IX and peaks 3 and 5 are due to configuration X.

We conclude from this analysis and the relative intensities of the curves in Figure 2 that the completely rearranged trimer contains about 75% of configuration X and 25% of configuration IX. This proportion agrees with that predicted assuming random statistics. If we arbitrarily assign the orientation of the =O and the OCH_3 groups as shown in configuration IX as A and the reverse orientation as B, in the trimer case the A's and B's can be arranged randomly three at a time according to the binomial expansion, i.e., $A^3 + 3A^2B + 3AB^2 + B^3$. The coefficient of each term corresponds to the number of ways the A's and B's can be arranged in that configuration. The A^3 and the B^3 arrangements are indistinguishable by NMR and correspond to configuration IX. Likewise, the remaining two terms are indistinguishable by NMR and correspond to configuration X. Therefore, for a random distribution of A and B orientations one would expect $^2/_8 = 25\%$ in configuration IX and $^6/_8 = 75\%$ in configuration X.

Furthermore, it appears that configuration X is composed entirely of two units of structure VI and one unit of structure VIII. Also, from the shift position and the relative intensity of peak 4, configuration IX is composed almost entirely of units of structure VII with possibly 5% of structure VIII included. This would explain the slightly higher value (~30%) for peak 5 in Figure 2. The X-ray study cited above[4] does not discuss the possibility of configuration IX, perhaps because of its low concentration. Intuitively one would expect the cis arrangement (configuration IX) to exist, and the ^{13}C spectra indicate that it is present, at least under the conditions of our experiments. Since the ^{13}C spectra were obtained at 120 °C or above, it is likely that the structures would be different from those found at room temperature by X-ray diffraction. It is also possible that two conformations of configuration X are being observed at the higher temperatures

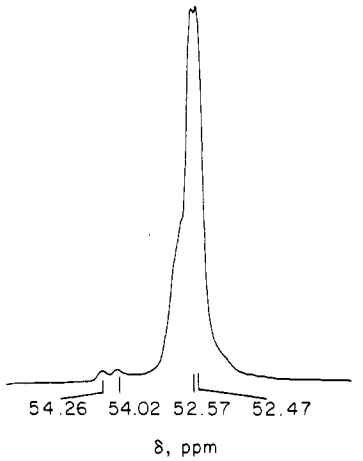

Figure 3. ^{13}C $\{^1H\}$ NMR spectrum of a relatively impure $[NP(OCH_3)_2]_3$ before heating. The figure shows "impurity" peaks due to incomplete derivatization.

of the ^{13}C measurement. However, room temperature solution ^{13}C spectra reveal the same three peaks in the same ratios. Therefore, we favor the first explanation.

Although the assignments of peaks 4 and 5 or 1 and 2 might possibly be reversed, the general conclusions are the same. Models of these trimers support the assignments and conclusions as stated. The conformations described allow for the most freedom of motion of the pendent groups. Rotation of the NCH_3 through the "plane" of the ring appears to be unlikely because of the partial double bond character of the P–N bonds.[4] Therefore, it seems reasonable that one conformation for each configuration (IX and X) would be predominant. At higher temperatures this might not be true.

^{31}P NMR. ^{31}P NMR can provide a wealth of information about phosphazene materials that is difficult or not possible to obtain by other means. All ^{31}P NMR spectra in this study are proton decoupled to eliminate long-range coupling effects. Because of the magnitudes of the coupling constants between phosphorus nuclei, the spectra can be very difficult to interpret. Nevertheless, we found it to be extremely useful both in confirming the ^{13}C NMR results and explaining "impurity" peaks observed in the ^{13}C NMR spectra. ^1H NMR was found to be not as useful in this case. There is now some evidence that the length of the "induction" period in the rearrangement might depend upon the level of the impurities. This will be discussed later.

Figure 3 illustrates an example of a trimer sample, the ^{13}C spectrum of which has two small, unexplained peaks at 54.26 and 54.02 ppm and a "hump" on the downfield side of the main peak. The ^{13}C NMR spectra of the purified, fully substituted trimer samples used in the thermolysis study did not have these extra peaks but displayed only a single peak with a small doublet splitting as expected. The small splitting (2.5 Hz) is the spin–spin coupling with the phosphorus nuclei.

The ^{31}P NMR solution spectrum of a similar trimer sample with a high impurity level is shown in Figure 4. It very clearly leads to an explanation of the extra peaks in Figure 3. Peak positions are referenced to 85% H_3PO_4. The prominent peak at 20.80 ppm is due to the fully substituted trimer as expected. The peak at 2.77 ppm is due to a small amount of fully substituted tetramer. This accounts for the hump on the side of the main peak in the ^{13}C NMR spectrum in Figure 3. The remaining eight peaks form a spin–spin coupling pattern characteristic of an AB_2 system. This means that one of the phosphorus nuclei in

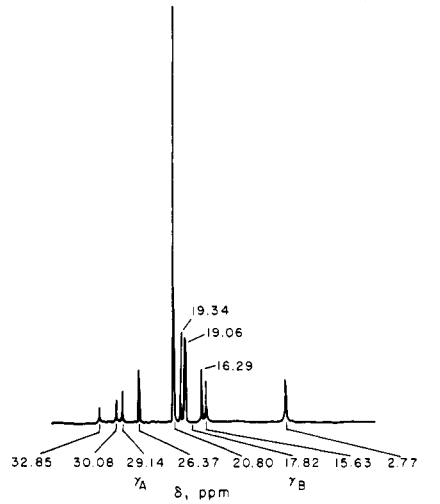

Figure 4. ^{31}P NMR solution spectrum of an incompletely derivatized trimer sample similar to that in Figure 3. Chemical shifts are referenced to external 85% H_3PO_4. Shows AB_2 pattern.

the trimer is differently substituted from the other two. Mass spectral analysis confirmed that the sample contained cyclochloropentamethoxyphosphazene, i.e., one of the chlorine atoms remained unsubstituted. This sample has a chlorine content of 4.3 wt %. Integration of the peak areas reveals that this sample contains 40.6 mol % of the pentasubstituted impurity and 4.5 mol % of tetramer. The two small peaks at about 54.1 ppm in the ^{13}C NMR spectrum of Figure 3 are due to the methoxy carbon which has a geminal chlorine. The remaining four methoxy carbons are buried under the main peak. Calculation of the composition based upon this assumption gives consistent results with those of the ^{31}P NMR spectrum.

Analysis of the AB_2 pattern[5] in Figure 4 gives the following parameters:

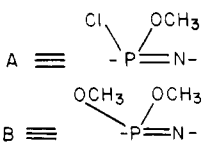

$$\nu_A = 29.14 \text{ ppm}$$

$$\nu_B = 17.82 \text{ ppm}$$

$$J_{AB} = 79.8 \text{ Hz}$$

$$(\nu A - \nu B)/J_{AB} = 0.292$$

Figure 5 is the ^{31}P NMR solution spectrum of the trimer sample of Figure 1 after having been heated sufficiently long (more than 3 h) at 140 °C for complete rearrangement. Two important conclusions can be drawn from this spectrum. First, all of the trimer molecules have experienced methyl migration. This is shown by the fact that all of the resonance has moved from 20 to about 7 ppm. Second, there appears to be a predominant AB_2 pattern in the resonance which could be used in support of either structure IX or X, depending upon which direction the NCH_3's are pointing. However, more careful analysis of the spectrum strongly suggests that it is really an ABC pattern.[6] This would favor structure X, in agreement with the ^{13}C results since the P nuclei in structure IX cannot generate an ABC spectrum. (Only A_3 or AB_2 patterns are possible.) Configuration X can generate either an AB_2 or an ABC pattern in the ^{31}P spectrum. There are four ways in which configuration X can lead to an ABC pattern, but it can be produced only if one of the two equivalent NCH_3's which are in conformation VI is locked in on one

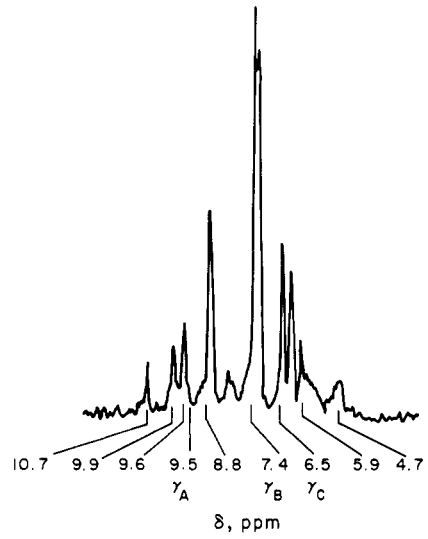

Figure 5. ^{31}P NMR solution spectrum of the trimer sample after heating for complete rearrangement.

side of the ring and the other is locked in on the other side. The two arrangements possible with these two methyls in opposite orientations are not distinguishable by ^{31}P NMR. Therefore, there are only two conformations of configuration X which would give an ABC pattern—one for each of the two orientations of the third NCH_3 on the ring.

A detailed computer simulation of this ABC pattern has been made. A quite good fit to the experimental spectrum is obtained with the following parameters assuming an ABC pattern:

$$\nu_A = 9.6 \text{ ppm}$$
$$\nu_B = 7.3 \text{ ppm}$$
$$\nu_C = 6.6 \text{ ppm}$$
$$J_{AB} = 20 \text{ Hz}$$
$$J_{AC} = 24 \text{ Hz}$$
$$J_{BC} = -30 \text{ Hz}$$

In Figure 5 there is excess resonance in addition to the main ABC pattern to account for the fraction of trimer molecules arranged as in configuration IX.

Cyclic Tetramer. ^{13}C NMR. The thermolysis of the dimethoxyphosphazene tetramer, XI, was studied over the

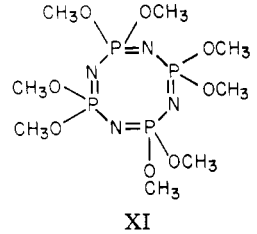

XI

temperature range 140–160 °C. Figure 6 shows ^{13}C NMR spectra of the tetramer at different stages of the rearrangement at 150 °C. As can be seen, the spectra are less complicated than those for the trimer case. The first peak appears at 33.04 ppm due to the monorearranged product. With continued heating, the major peak develops at 33.66 ppm. When the rearrangement is complete, only a single peak remains in the NCH_3 region. A corresponding peak develops in the methoxy region at 54.43 ppm.

This interesting result indicates that the rearranged product has a regular structure and has but one configuration. As was mentioned briefly in the discussion of the trimer, the rates of rearrangement for the third and fourth methyl migrations must be fast compared with those of

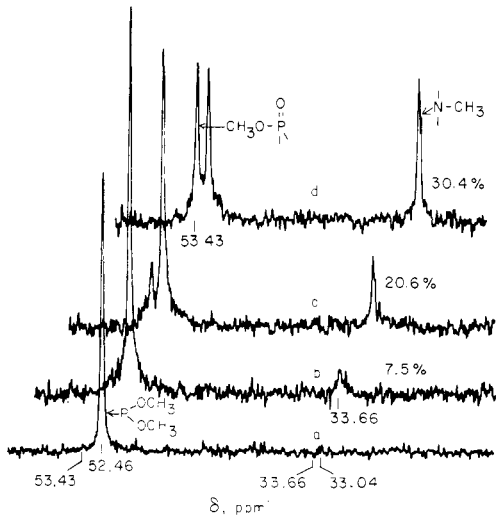

Figure 6. ^{13}C $\{^1H\}$ NMR spectra at 25.14 MHz of the thermolysis of $[NP(OCH_3)_2]_4$ at 150 °C. Spectra were run on a neat sample in a sealed, evacuated tube with a repetition time of 28 s and a 45° pulse. (Longest T_1 = 10 s at 150 °C.) Peak positions are referenced to Me_4Si. The percentages of the methyl groups which have migrated to the nitrogen are given above the spectra: (a) before heating; (b) after 3 h; (c) after 4 h; (d) after 5 h.

the second because we do not observe the intermediate peaks as in the trimer case. We do observe a peak associated with the initial methyl migration, however. This disappears in the latter stages.

The only configurations that would give a single NCH_3 peak are shown in structures XII, XIIA, and XIII. Again,

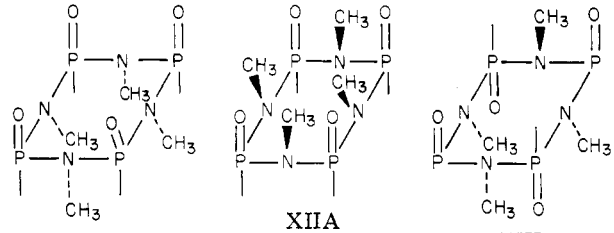

XII XIIA XIII

these structures do not show correct bond angles but are sketched to show the relative positions of the P=O. The CH_3O groups are omitted to reduce clutter. The other two configurations possible would lead to more than a single NCH_3 peak. There are several arrangements possible for the NCH_3's in configuration XIII, but all of them are equivalent from the standpoint of the NCH_3 resonance.

Another possible explanation for the observation of a single NCH_3 peak would be a rapid inversion of the methyl groups. However, spectra obtained at lower temperatures fail to show a splitting or a broadening of the peaks as would be expected for a hindered rotation. It would be very difficult for the nitrogen methyl groups to rotate above and below the ring because of the partial double bond character of the P–N bonds. Therefore, one conformation is probably locked in. Because of the observation of only one NCH_3 peak, configuration XII is restricted to the two possibilities that all of the NCH_3's are either in conformation VII (anti to P=O) as shown in XII or conformation VIII (syn to P=O) as shown in XIIA. The molecular models rule out XIIA because of steric hindrance. However, XII allows considerable freedom of movement.

Therefore, the ^{13}C NMR spectra suggest that the completely rearranged tetramer has only one configuration—either configuration XII with all nitrogen methyls anti to P=O or structure XIII in which alternate P=O groups

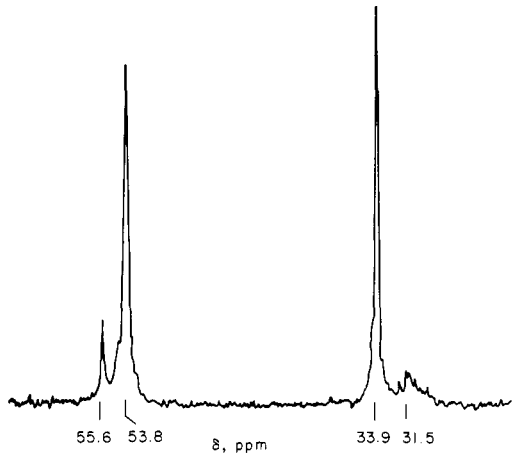

Figure 7. ^{13}C $\{^1H\}$ NMR spectrum of the tetramer after heating 24 h at 160 °C. The figure shows the start of a further rearrangement or decomposition after the methyl migration is completed. The spectrum was obtained at 26 °C with $CDCl_3$ as the solvent.

have the same orientation. The latter is more likely.

If the rearranged product is heated for long periods of time, a second rearrangement takes place. This is seen in Figure 7 in which the sample is heated at 160 °C for 24 h. A new peak appears in the methoxy region at 55.60 ppm and a broad resonance appears at 31.5 ppm. This spectrum was run with $CDCl_3$ as the solvent because of the broadness of the lines in the bulk spectrum. The peak at 55.60 ppm increases at the expense of the methoxy peak at 53.82 ppm. This undoubtedly is the result of a change in conformation to a more thermodynamically stable form. Two isomers of the phosphazane tetramer have been characterized previously.[7] One isomer, mp 216–218 °C, has a 2-trans-4-cis-6-trans-8 structure, i.e., configuration XIII; its ring has a slightly distorted boat conformation. The other isomer, mp 212–214 °C, has a 2-cis-4-trans-6-trans-8 structure; its ring has a chair conformation. The ^{13}C NMR spectrum agrees with the former isomer before the transformation takes place, but it does not explain the latter isomer after the transformation. This suggests that only a conformation change is taking place. This phenomenon will not be discussed further in this paper.

^{31}P NMR. The ^{31}P NMR spectrum of the tetramer before heating is a sharp, single peak at 3.00 ppm (wrt 85% H_2SO_4) which is shifted to 8.17 ppm after heating. This confirms the conclusion from ^{13}C NMR that the rearrangement product has only one configuration. Either of the two configurations discussed in the above section would lead to a single ^{31}P peak, so we cannot distinguish between them. The single peak eliminates the 2-cis-4-trans-6-trans-8 isomer mentioned above as a possibility because this would exhibit an AA'BB' pattern in the ^{31}P spectrum.

Polymer. ^{13}C NMR. Qualitatively, the ^{13}C NMR spectra of the thermolysis of the dimethoxy polymer are similar to those of the tetramer shown in Figure 6. Quantitatively, the rate is much faster, as will be seen in the next section. Figure 8 shows solution spectra at various stages of the rearrangement. The bulk spectra peaks are broader and hence show less detail. As the rearrangement approaches completion, the NCH_3 peak is essentially a singlet as in the case of the tetramer. This indicates that the rearranged polymer also has a very regular structure. All units are either in the form of structure VI, which in terms of the phosphorus pendant groups would be analogous to a syndiotactic structure, or in the form of structure VII or VIII, which would be analogous to an isotactic structure. In contrast to the tetramer case where steric

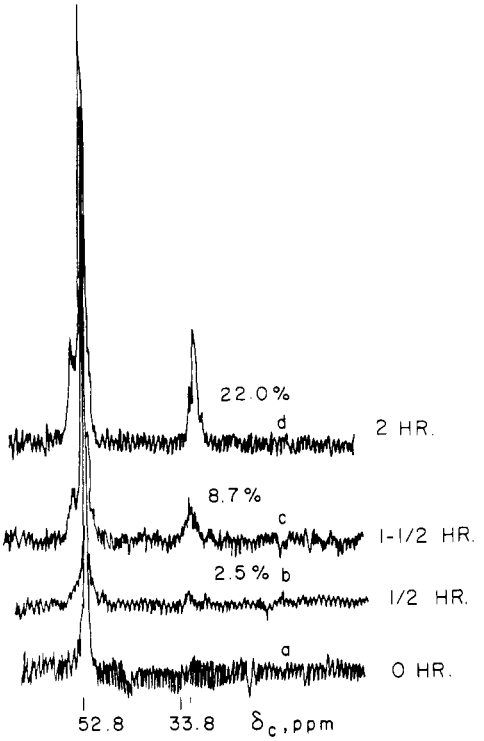

Figure 8. ^{13}C $\{^1H\}$ NMR solution spectra at 25.14 MHz of thermolysis of poly(dimethoxyphosphazene) at 140 °C. The longest T_1 = 0.6 s at 140 °C for the bulk polymer. Samples were first heated in the bulk but were then dissolved in $CDCl_3$ for the NMR measurement. The peaks in the bulk spectra are too broad to reveal fine structure details: (a) before heating; (b) after 0.5 h; (c) after 1.5 h; (d) after 2 h.

Table II
Nuclear Overhauser Enhancement for the Cyclodimethoxyphosphazene Trimer

	OCH_3		NCH_3	
peak position, ppm	52.50	54.09	33.08	30.95
120 °C	2.53	1.94	2.53	2.46
130 °C	2.45	2.23	2.64	2.58
140 °C	2.32	2.24	2.66	2.30

hindrance very likely excludes structure VIII, in the polymer case this restriction probably does not apply. However, the facts that there is but a single peak and the chemical shift is the same as that of the tetramer suggest that structure VIII is not present in the polymers.

^{31}P NMR spectra of the completely rearranged polymer were not obtained because cross-linking renders the product insoluble.

Kinetic Study

Nuclear Overhauser Enhancement (NOE) which results from the decoupling of the protons from the ^{13}C nuclei can lead to serious quantitative errors if not taken into account. In general, each carbon nucleus will have a different NOE, so for quantitative measurements it is important either to know the NOE of each type of carbon nucleus and then to correct for it or to eliminate it. We have done both. In some of the early work the NOE was measured for each peak by comparing the integrated intensities of the peaks run in the decoupled mode (normal spectrum) with those run in a gated decoupling mode in which the NOE was eliminated. NOE values for the major peaks in the spectrum of the cyclic trimer are given in Table II. Calculations based upon these spectra were corrected for the NOE's. A more convenient method is to run the spectra in the gated decoupling mode which eliminates it

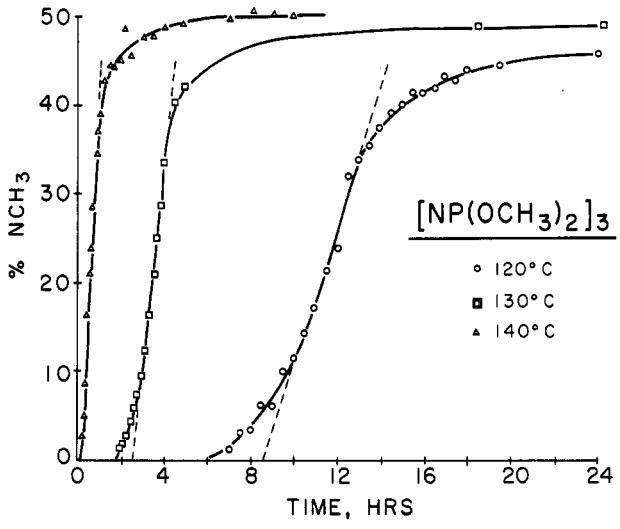

Figure 9. The percent of total methyl groups which have migrated to the nitrogen vs. time for $[NP(OCH_3)_2]_3$ at three temperatures.

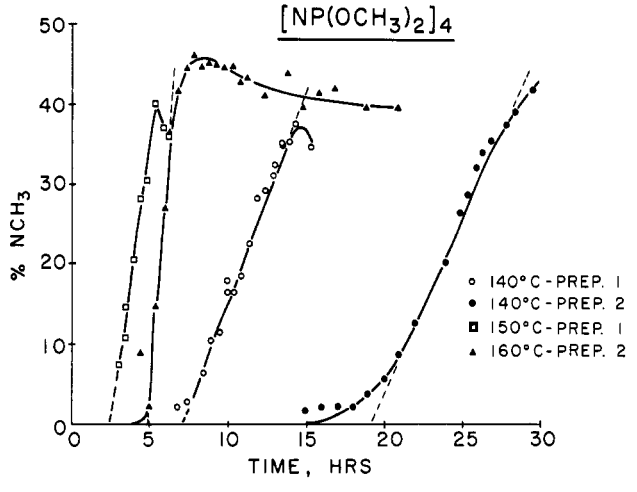

Figure 10. The percent of total methyl groups which have migrated to the nitrogen vs. time for $[NP(OCH_3)_2]_4$ at three temperatures. Note that at 140 °C two different preparations result in two curves which are considerably separated from each other.

entirely; thus the intensities can be used without correction. Much of the data was obtained in this mode.

The effect of time and temperature upon the migration reaction is shown in Figures 9–11 for the trimer, tetramer, and polymer, respectively. Figure 12 is a comparison of the trimer, tetramer, and polymer heated at a constant temperature of 140 °C. In these curves, the total number of methyl groups that have migrated to nitrogen atoms, taken as the sum of peaks in the N–CH_3 area, is plotted against the time of heating. "S" shaped curves are obtained, indicative of several reactions occurring simultaneously or consecutively. Definite induction periods, that depend upon the temperature of heating, are present. The initial reaction is autocatalytic, starting slowly and generating species that are involved in the migration of the methyl group until it reaches a constant or maximum rate. This behavior is common to all three compounds.

Figure 10 shows the data for two separate preparations of the dimethoxy tetramer. These two preparations behaved differently in that the number two preparation exhibited a much longer induction period than the number one. Thus, adventitious factors are operative during the heating. Some possibilities are the presence of extraneous

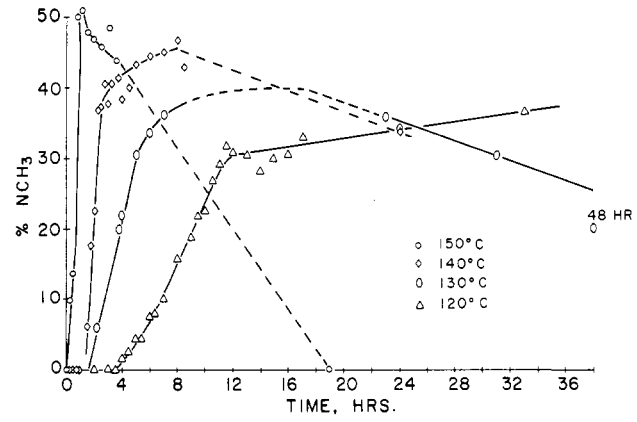

Figure 11. The percent of NCH_3 vs. time for poly(dimethoxyphosphazene) at four temperatures.

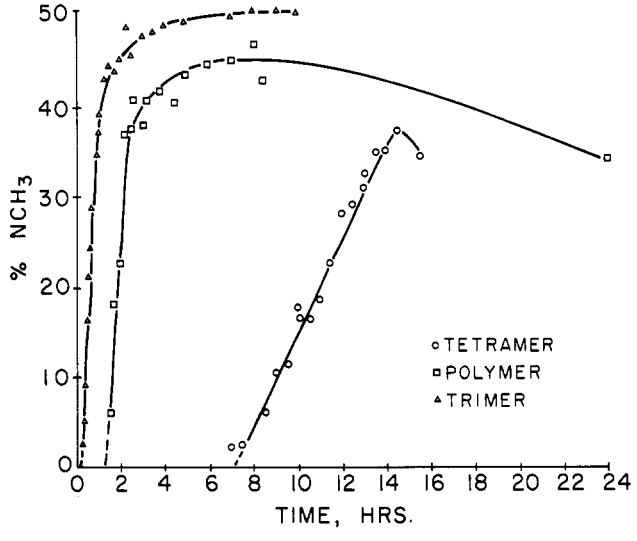

Figure 12. Comparison of thermolysis rates of the trimer, the tetramer, and the polymer at 140 °C.

impurities remaining from the derivatization reactions or small concentrations of fortuitous groups attached to the tetramer ring structure. The second preparation was obviously purer than the first which poses the question of the ultimate stability of a rigorously pure sample.

In the latter stages of the reaction, the behavior of the trimer is quite different from that of the tetramer and polymer. The percentage of methyl groups attached to nitrogen actually goes through a maximum and decreases in the case of the latter two structures while for the trimer it approaches 50% and remains constant with additional heating (44 h at 120 °C). This decrease in nitrogen methyl, late in the reaction, is due to crystallization in the case of the tetramer and possibly partial recrystallization and cross-linking in the case of the polymer. The tetramer forms a white crystalline solid which is undoubtedly the phosphazane. The polymer goes through the stages of solid, to fluid, to viscous liquid, to a solid resinous material or partially crystalline material which is insoluble. In addition to the polymer phosphazane formation and scission, a cross-linking reaction must be taking place. The trimer has also formed the phosphazane structure, but it remains in the liquid state at temperatures above 120 °C. The crystalline fraction in the tetramer or the polymer or the resinous material in the polymer would not be observable by ^{13}C NMR without special techniques. Therefore, the NMR signal intensity of the rearranged species would be expected to decrease with respect to the unrearranged species for the tetramer and the polymer.

Table III
Methyl Migration Rate Constants (%/h)

	120 °C	130 °C	140 °C	150 °C	160 °C	E, Kcal
$[N\text{-}P(OCH_3)_2]_3$	9.55	27	54-61			32.1
$[N\text{-}P(OCH_3)_2]_4$			5.2	14.1		34.5
			4.2		25.0	31.9
$[N\text{-}P(OCH_3)_2]_x$	4.15	9.05	31	51-55		30.6

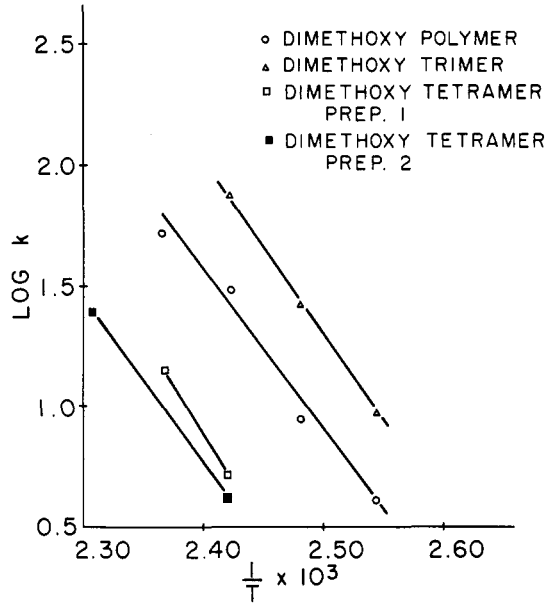

Figure 13. Plot of the log of the rate vs. $1/T$ for the trimer, the tetramer, and the polymer.

Due to the "S" nature of the kinetic curves, the rate of the migration starts out very slowly, gradually increases, reaches a maximum, and then gradually decreases. However, the rate, as determined by the slope of the curves, is fairly constant for a large percentage of the reaction. This constant slope, as indicated by the dotted curves in Figures 9–10, was determined for each curve and listed in Table III.

The logarithm of these values for the slopes is plotted against the reciprocal of the absolute temperature in the usual manner in Figure 13. The slopes of these lines were converted to the activation energy values as shown in the last column of Table III. The variation in these values is certainly within experimental error even for the two preparations of tetramer, so it appears that the activation energy is the same for the three compounds, and migration of the methyl occurs by the same reaction coordinate. The differences in the individual rate constants must be due to differences in the front factors. In terms of thermodynamics, the activation enthalpies are the same but the entropies are different.

It is observed that the polymer liquefies during the heating and the subsequent migration of the methyl group to the nitrogen atoms. In fact, the polymer viscosity decreases sharply with little or no detectable migration by NMR. The solution viscosities of the dimethoxy polymer and two others which contain methoxy as one substituent but trifluoroethoxy or phenoxy as the other substituent were followed as a function of the time of heating at 140 °C. The data are listed in Table IV. More detailed kinetic data of these other polymers will be published later in part 3 of this series of papers. Their viscosity data are included here to provide more experimental support for our contention (described below) that there is a correlation between the methyl migration and the number of scissions

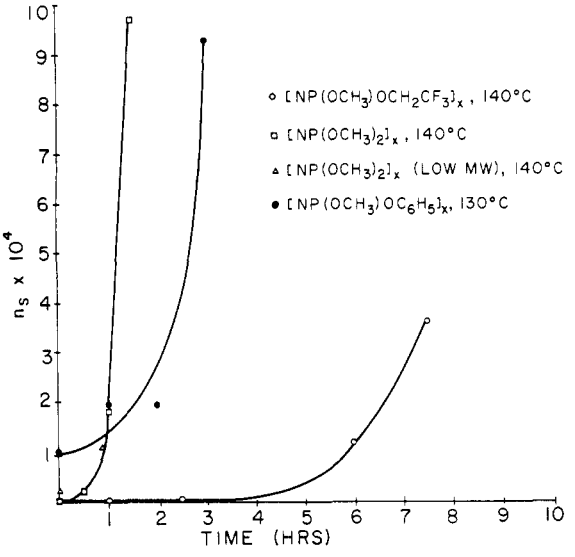

Figure 14. n_s vs. time from viscosity measurements for three polymers. n_s is the number of scissions.

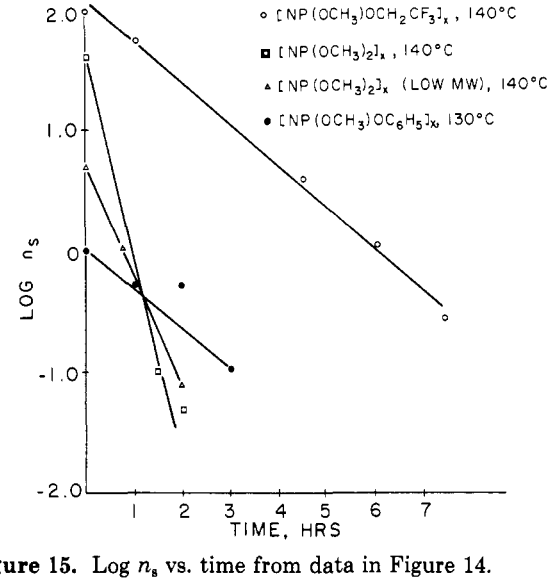

Figure 15. Log n_s vs. time from data in Figure 14.

of the chain. These data were converted to molecular weight data by using eq 1,[8] where η is the viscosity, and

$$\eta = (3.60 \times 10^{-3})M^{0.5} \quad (1)$$

M is the molecular weight. This, at best, is a crude attempt to estimate the amount of degradation that occurs during the heating. The actual number of scissions, n_s, was then calculated as

$$n_s = 2/M \quad (2)$$

where the factor of 2 represents approximately the ratio between the viscosity average and number average molecular weight of randomly degraded polymer. Most of the derivatized polyphosphazene polymers have a M_w/M_n ratio of approximately 2, characteristic of Flory's most probable distribution, prior to heating. It is believed that this scission reaction takes place in a random fashion so that this ratio would not change drastically during the reaction. If these concepts are correct, the use of the factor 2 in eq 2 is justified.

These estimated values of the number of scissions occurring during the heating are plotted in Figure 14 as a function of time. Figure 15 is a semilogarithmic plot which shows the exponential nature of the data. The change in viscosity is an extremely sensitive indicator of the scissions

Table IV
The Effect of Heating upon Solution Viscosity of Polymers at 140 °C

I. $[NP(OCH_3)_2]_x$

	time, h	% NCH_3	$\eta_{25\,°C}$ ($CHCl_3$)
polymer A	0	0.0	2.25
	0.5	0.0	0.75
	1.0	2.5	0.27
	1.5	8.6	0.13
	2.0	22.0	0.06
polymer B	0.0	0.0	0.81
	0.82	0.0	0.35
	2.0	22.0	0.1
	3.0	39.5	

II. $[NP(OCH_3)(OCH_2CF_3)]_x$

time, h	% NCH_3	η_{25}°C(THF)
0.0	0.0	3.68
1.0	0.0	2.69
2.5	0.0	2.51
4.5	0.5	0.72
6.0	2.7	0.34
7.5	4.8	0.19
24.0	28.8	0.03

III. $[NP(OCH_3)(OPh)]_x$

time, h	% NCH_3	η_{25}°C(Tol)	η_{25}°C(THF)
0.0	0.0	0.38	0.54
1.0	1.7	0.26	-
2.0	6.8	0.26	0.36
3.0	10.8	0.15	-
5.0	18.1	0.08	0.11

that occur. Thus, it would appear that the scission reaction starts immediately at the beginning of the heating and increases exponentially during the so-called induction period as measured by NMR.

It is of interest to compare the viscosity with the NMR data. To do this, the NMR data were converted to moles of CH_3 migrated per gram of polymer, and the results are shown in Figure 16 where moles of scission are plotted against moles of migration. The straight line indicates a one to one correspondence. The questionable procedure utilized in obtaining the scission data should be pointed out again. However, the number of scissions occurring is certainly of the same order of magnitude as the number of migrations, and the agreement suggests that they may be related in some manner. It should be remembered that this is not the situation in the case of the trimer where the methyl group migrates with no measurable scission of the ring.

Discussion

Any mechanism of the thermolysis of $[NP(OCH_3)_2]_n$ would have to explain the following observed features: (1) induction period; (2) autocatalytic behavior; (3) scissions (polymer); and (4) cross-linking (polymer). The mechanism we propose does account for them somewhat satisfactorily. Although there is considerable speculation in some of the steps, there is strong experimental evidence for certain others.

Induction Period. The length of the induction period is apparently related to the purity of the material. The impurities are probably incompletely derivatized phosphorus sites which have chlorine or OH attached as represented in eq 3 and are responsible for initiating the

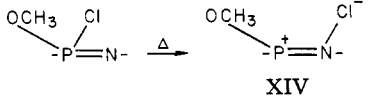

XIV (3)

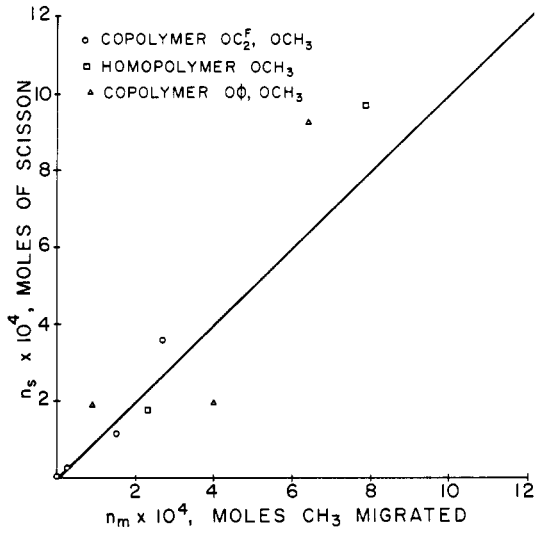

Figure 16. Correlation of the number of chain scissions (n_s) from viscosity measurements with the number of moles of methyl migration (n_m) from NMR measurements.

rearrangement. The reactions shown apply to trimer, tetramer, or polymer except where noted. Once initiated by eq 3, the rearrangement can proceed by either an intramolecular or an intermolecular attack as shown by the following equations.

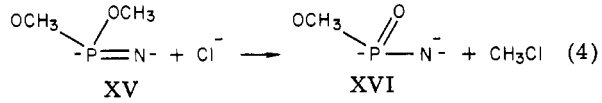

XV XVI (4)

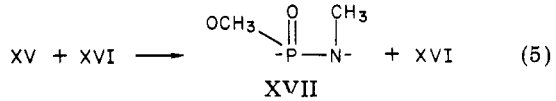

XVII (5)

Support for eq 4 is given by the fact that mass spectral analysis detects CH_3Cl as the predominant gaseous component when the sealed tubes are broken open after rearrangement is completed. The effect of methyl chloride on the rate of the reaction is not clear. It is also possible that a certain amount of intermolecular coupling could take place through the nitrogen.

Autocatalytic Behavior. The steps listed above would not explain the autocatalytic nature of the rearrangement but would be restricted by the concentrations of the impurities. Autocatalysis of the reaction could arise from the following steps either intra- or intermolecularly:

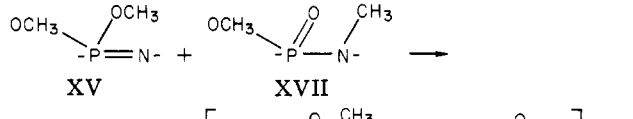

XV XVII

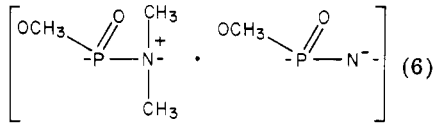

(6)

XVIII

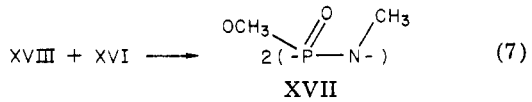

XVII (7)

Thus, 2 mol of XVII are formed for each one present as a reactant in eq 6, and hence the reaction proceeds autocatalytically. The rate increases as the concentration of XVII increases. Therefore, we are suggesting that the rearranged product, XVII, behaves as a catalyst.

Scissions (Polymer). Upon complete rearrangement the trimer and the tetramer are converted to the corre-

sponding phosphazanes, which are white crystalline solids. The polymer, however, first breaks down into a fluid liquid, and later in the reaction it sets up into an insoluble resinous mass through some means of cross-linking and possibly a crystallization. As was discussed in the previous section, the rate of scission has roughly a one-to-one correspondence with the methyl migration. To account for the scission process of the polymer, we suggest the following mechanism:

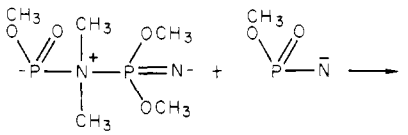

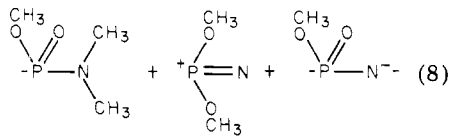

(8)

XIX

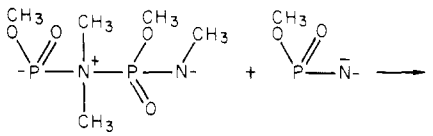

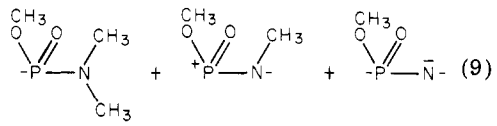

(9)

XX

(10)

If there is a scission for every methyl migration, then as the rearrangement goes to completion, there should be a great deal of low molecular weight amine present. In fact, if it were not for the apparent cross-linking, in the latter stages the product should be composed mostly of simple phosphoamines with one P and one N. Mass spectral analysis confirms the presence of major amounts of amines when the sealed reaction tube is opened. Also, small, oily drops of liquid are deposited above the main mass of the rearranged polymer in the reaction tube. These liquid drops turn litmus paper red, indicating a phosphoric acid has been formed as postulated in eq 10. The extent of this reaction should be quite small because of the limited amount of H_2O in a sealed, evacuated tube.

Cross-Linking (Polymer). To account for the observation that the polymer changes from a low viscosity liquid, to a viscous liquid, and to a resinous solid with continued heating, a number of cross-linking reactions could be taking place. We have no experimental evidence for any particular path, but we suggest eq 11 as a possibility. In this case P–O–P cross-links are formed, but pathways can also be imagined in which P–N–P cross-links are formed. There is a great deal of speculation in the mechanism proposed above, but in general, it appears to be reasonable and consistent with the experimental facts observed during the course of the rearrangement.

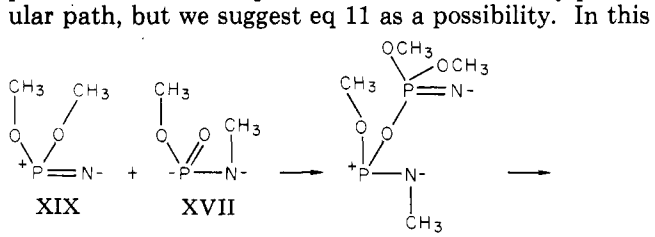

XIX XVII

cross-linking (11)

Conclusions

The migration of the methyl group in the thermolysis of dimethoxyphosphazenes is conveniently followed by ^{13}C NMR in the bulk samples. All of the intermediate stages of rearrangement are readily observed in the trimer. Upon complete rearrangement of the trimer a random distribution of the two possible configurations is observed. However, within each configuration there appears to be only one conformation allowed at the temperature studied. The tetramer and the polymer both have but one configuration, and it appears to be the same—either isotactic or syndiotactic with respect to the P=O.

^{31}P NMR confirms the above conclusions but provides additional information. The spin–spin coupling patterns can be used to confirm the conformations and the configurations of the rearranged products. It is also useful for identifying the underivatized phosphorus-containing impurities.

The kinetic data showed that there is an induction period and the rearrangement is autocatalytic. The induction period was related to the impurities of Cl or OH on incompletely derivatized phosphorus sites. Activation energies over the straight line portions of the kinetic curves are the same within experimental error for trimer, tetramer, and polymer, showing that the methyl migration proceeds by the same reaction coordinate.

A mechanism was proposed which can explain the induction period and the autocatalytic behavior of all three species. An additional mechanism is suggested to account for the scissions and the cross-linking observed in the polymer. It was found that there is roughly a one-to-one correspondence of the methyl migration and the number of scissions.

Acknowledgment. The authors wish to acknowledge helpful discussions with T. A. Antkowiak and the permission of The Firestone Tire & Rubber Company to publish this article.

References and Notes

(1) M. E. Mirhij and J. F. Henderson, *J. Macromol. Chem.*, 1, 187 (1966).
(2) V. D. Mochel and T. C. Cheng, *Macromolecule*, 11, 176 (1978).
(3) L. F. Johnson and W. C. Jankowski, "Carbon-13 NMR Spectra", Wiley, New York, 1972, spectrum No. 221.
(4) G. B. Ansell and G. J. Bullen, *J. Chem. Soc. A*, 3026 (1968). This reference was suggested by a reviewer.
(5) J. A. Pople, W. G. Schneider, and H. J. Bernstein, "High Resolution Nuclear Magnetic Resonance", McGraw-Hill, New York, 1959, pp 123–128.
(6) F. A. Bovey, "Nuclear Magnetic Resonance Spectroscopy", Academic Press, New York, 1969, p 313.
(7) R. A. Shaw, *Phosphorous Sulfur*, 4, 101 (1978).
(8) This relationship has been developed and used at the Central Research Laboratories of The Firestone Tire and Rubber Company based upon unpublished data.